
PARKINSON'S DISEASE DIAGNOSIS BASED ON GAIT CYCLE ANALYSIS THROUGH AN INTERPRETABLE INTERVAL TYPE-2 NEURO-FUZZY SYSTEM

A PREPRINT

Armin Salimi-Badr

Faculty of Computer Science and Engineering
Shahid Beheshti University
Tehran, Iran
a_salimibadr@sbu.ac.ir

Mohammad Hashemi

Faculty of Computer Science and Engineering
Shahid Beheshti University
Tehran, Iran
mohamm.hashemi@mail.sbu.ac.ir

Hamidreza Saffari

Faculty of Computer Science and Engineering
Shahid Beheshti University
Tehran, Iran
h.saffari@mail.sbu.ac.ir

March 14, 2022

ABSTRACT

In this paper, an interpretable classifier using an interval type-2 fuzzy neural network for detecting patients suffering from Parkinson's Disease (PD) based on analyzing the gait cycle is presented. The proposed method utilizes clinical features extracted from the vertical Ground Reaction Force (vGRF), measured by 16 wearable sensors placed in the soles of subjects' shoes and learns interpretable fuzzy rules. Therefore, experts can verify the decision made by the proposed method based on investigating the firing strength of interpretable fuzzy rules. Moreover, experts can utilize the extracted fuzzy rules for patient diagnosing or adjust them based on their knowledge. To improve the robustness of the proposed method against uncertainty and noisy sensor measurements, Interval Type-2 Fuzzy Logic is applied. To learn fuzzy rules, two paradigms are proposed: 1- A batch learning approach based on clustering available samples is applied to extract initial fuzzy rules, 2- A complementary online learning is proposed to improve the rule base encountering new labeled samples. The performance of the method is evaluated for classifying patients and healthy subjects in different conditions including the presence of noise or observing new instances. Moreover, the performance of the model is compared to some previous supervised and unsupervised machine learning approaches. The final Accuracy, Precision, Recall, and F1 Score of the proposed method are 88.74%, 89.41%, 95.10%, and 92.16%. Finally, the extracted fuzzy sets for each feature are reported.

Keywords: Parkinson's Disease, Interval Type-2 Fuzzy Neural Networks, Interpretable Artificial Intelligence, Gait Cycle.

1 Introduction

Emerging symptoms of some chronic diseases like Parkinson's Disease are diagnosed many years after infection. This delay reduces the chance of encountering the disease with some more simple treatment methods. Parkinson's disease (PD) is the second most common neurological disease that puts the lives of a large portion of the elderly population in danger [35, 24, 49]. This slow and progressive neurodegenerative disorder is the consequence of destroying dopaminergic neurons in the Substantia Nigra pars compacta, one nucleus of a complex subcortical brain structure named

Basal Ganglia [22, 56, 57, 35]. According to the Parkinson's disease foundation, Most PD patients show movement disorders including movement slowness (Bradykinesia), impairment of the power of voluntary movements (Akinesia), rigidity, and resting tremor [22]. Near 5 million people are affected by PD in the world [35]. The age-standardized mortality rate in Iran is reported about 3.44% [17].

It would be possible to control and decrease the syndromes by medical treatments or changing lifestyles in the early stages of the disease. However, by progressing this illness, more complex and aggressive approaches including surgical therapy like using Deep Brain Stimulus (DBP) are required. Unfortunately, the PD begins 5 to 10 years before appearing any clinical symptoms [35]. Moreover, some non-typical signs such as depression, pain, fatigue, etc. could make the diagnosis more difficult. Generally, the diagnosis task is difficult based on the reported misdiagnosis rate of 25% of cases [11]. Machine learning, ambient intelligence, and context-aware agents can help us to improve the quality of healthcare services and disease diagnosis.

Two important symptoms, studied in the previous methods to classify the patients and healthy persons are *speech disorders (vocal impairment)* [11, 3, 24] and *gait cycle changing* [35, 34, 58]. Since PD affects mainly the patient's movements by disorders like rigidity, Bradykinesia, Akinesia, tremor, and difficulty with balance and coordination its effects on the gait cycle are expected.

Most previous approaches that applied machine learning paradigms for classifying patients suffering from PD have not used either an interpretable artificial intelligence method [35, 34] or they not used expert understandable clinical features [58, 37, 45]. However, in a sensitive clinical application, using an interpretable method with clinical features is more acceptable for two reasons: 1- An expert can verify the decision of the model, and 2- an expert can modify and fine-tune the parameters of the model.

In this paper, an interpretable artificial intelligence-based approach using the clinical features extracted from the gait cycle is proposed. The paradigm is based on training an interpretable interval type-2 fuzzy neural network and applying a hybrid batch-online learning method. First, high-level features explaining the behavior of the gait cycle obtained from wearable sensors are extracted. Next, using available training instances, an interval type-2 fuzzy neural network with interpretable structure is trained. Based on training this interpretable structure, some fuzzy rules are extracted which can be used as a guide for experts to diagnose patients. On the other hand, experts can modify and fine-tune the parameters of extracted fuzzy rules based on their knowledge.

Moreover, sensors measure noise along with the target signal. Therefore, using the interval type-2 fuzzy logic increases the robustness of the extracted fuzzy rules against the noisy data. Considering the progress of studies and collecting more labeled instances in the future, a complementary online learning method is proposed to add new fuzzy rules encountering new training samples. The main contributions of our proposed method are summarized as follows:

1. Presenting an interpretable model based on clinical features. Therefore, the decisions made by the model can be verified by the experts. Moreover, extracted rules can be used by experts or be adjusted based on the experts' knowledge;
2. Increasing the robustness of the method against uncertainty and sensor noisy measurements using Interval Type-2 Fuzzy logic;
3. Proposing an initial batch learning to extract fuzzy rules based on available training samples and proposing complementary online learning for improving the model's rule base using new labeled instances;
4. Avoiding local search like Gradient Descent for tuning network's parameters. Using local search optimizations could lead overfitting.

The rest of this paper is organized as follows: First, in section 2 the related studies are reviewed. Afterward, in section 3 the proposed paradigm including the utilized features, preprocessing, the proposed Interval Type-2 Fuzzy Neural Network architecture, and learning algorithms are explained. Next, the results on some labeled data are reported and compared with some other methods that used similar clinical features in section 4. At the end of section 4, the extracted fuzzy sets are reported. Finally, conclusions are presented in section 5.

2 Related Work

The deterioration of executive functions and movement disorders in patients with PD have been shown extensively [39, 42, 4]. Yogeved et al. [62] studied the impacts of different types of dual-tasking and cognitive function on the gait of patients with PD and control subjects. They also showed contrasting measures of gait rhythmicity for patients with PD in comparison to other features. Additionally, in [63] it is investigated that Parkinson's disease has a great impact on the left-right symmetry of gait. Yogeved et al. [63] conducted a similar walking condition for both patients with

PD and healthy control subjects and they demonstrated that asymmetry of gait increased mainly during the dual-task condition in patients with PD but not in the healthy control subjects. Considering the Hausdorff et al. [26] studies on gait variability and Basal Ganglia disorders, it can be concluded that the ability to maintain a steady gait with low stride-to-stride variability of gait cycle timing, would be decreased in patients with PD. Parkinson's disease symptoms also include speech disorders as well as cognitive impairments [48, 23]. In addition, 90% of the patients with PD themselves report speech impairments as one of the most significant symptoms [25].

To classify the patients with PD and healthy control subjects based on their gait cycles, both wearable [31, 2, 46, 29, 50, 51, 41] and non-wearable [36, 9, 47, 21, 13, 14, 1, 59, 18, 44, 61] sensors have been used in various experiments. For instance, Jean et al. [31], conducted the classification using Spatial-Temporal Image of Plantar pressure (STIP) among normal step and patient steps with PD. In [41] Mariani et al. presented a technology based on wearable sensors on-shoe and utilizing algorithms, which had an outcome of characterizing Parkinson's disease motor symptoms during 'Timed Up and Go' (TUG) and gait tests.

Accordingly, the classification of healthy control subjects and patients with PD using ground reaction force sensors placed in shoes has been extensively studied [60, 64, 10, 37, 58, 34, 35]. In [10], the vGRFs measurements of both left and right foot were used to extract statistical features including minimum, maximum, average, and the standard deviation of each time series. Their extracted features then were fed to machine learning binary classifier including Support Vector Machine (SVM). In [60] Su et al., the gait asymmetry (GA) was calculated by comparing the ground reaction force (GRF) features of the left and right limbs. This was done by decomposition of the GRF into components of different frequency sub-bands via the wavelet transform and Multi-Layer Perceptron (MLP) models. In [37], Lee et al. utilized the gait characteristics of idiopathic PD patients who shuffle their feet while they are walking to classify patients with PD and healthy control subjects. They trained a neural network with weighted fuzzy membership functions (NEWFM) using extracted 40 statistical and wavelet-based features.

Different supervised and unsupervised methods such as Decision Tree (DT), Support Vector Machine (SVM), K-Nearest Neighbors (KNN), Gaussian-Mixture Model (GMM), and K-Means are extensively utilized to classify patients with PD and healthy control subjects. In [32], automatic noninvasive identification of PD is used with the combination of wavelet analysis and SVM which led to an accuracy of 90.32%. Although most of the previous studies are mainly based on the use of time-domain and frequency-domain features, in [35], only the clinical-based features extracted from vertical Ground Reaction Forces (vGRFs) were considered. Accordingly, nineteen statistical features measuring different aspects of the gait cycle are extracted and used as the input of machine learning-based classifiers. However, most of the previous works tried to extract feature vectors based on some human knowledge, in [58], demonstrated that the spatial correlation among different sensors data during time placed in each left and right foot are useful for diagnosing the patients. To consider the temporal dependencies, they proposed a structure that has Long-Short Term Memory (LSTM) cell layers to build a Recurrent Neural Network (RNN).

A time-delay neural network classifier learned by a Q-back propagation learning approach was proposed in [45] using temporal information of vGRF time-series to predict the severity of gait disturbances in subjects with PD. The dataset used includes data from three PD research studies [62, 20, 27]. The results show that the classification accuracy on the three sub-datasets reached 91.49%, 92.19%, and 90.91%, respectively.

Most previous studies have not used clinical features or have not applied an interpretable method for classifying PD patients. Using an interpretable machine learning approach that the base of its decision making is transparent and expert understandable is more agreeable in a clinical application. Fuzzy Neural Networks are interpretable structures with neural representation [30, 12, 15, 16, 55, 53, 54, 52]. In this study, the clinical features which are understandable for experts are extracted from the recorded vGRF signal and an interpretable structure, based on Interval Type-2 Fuzzy Neural Network is utilized to classify subjects using these clinical features. Consequently, contrary to the previous studies that used clinical features with non-interpretable machine learning methods like [35], or used sequence of vGRF like [37], the proposed method is able to extract expert understandable rules. These rules can be verified and modified based on the knowledge of experts. On the other hand, experts can utilize the extracted rules to detect patients suffering from PD.

3 Materials and Methods

In this section, we explain the proposed method including the preprocessing, the architecture of the Interval type-2 Fuzzy Neural Network, the algorithm to learn its parameters, and finally a complementary online learning for improving the method encountering new labeled examples. Figure 1 shows the whole proposed paradigm of this article. In the following subsections, different parts of this paradigm will be explained.

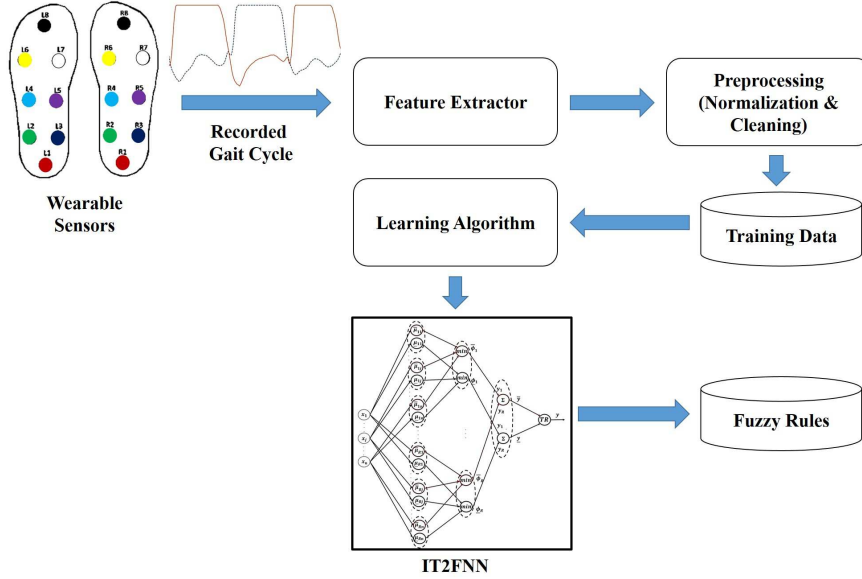


Figure 1: The proposed paradigm in a single view. First, the gait cycle in the form of vertical Ground Reaction Force (vGRF) is extracted from some wearable sensors during subject's walking. Afterward, the recorded vGRF signals are preprocessed. Next, clinical features are extracted from the recorded vGRF signals and the training samples are constructed. Using the training samples, an Interval Type-2 Fuzzy Neural Network is trained based on a batch learning algorithm and some fuzzy rules are extracted.

3.1 Features and Preprocessing

The gait cycle is composed of two phases (3) [35, 34]: stance phase (60% of the gait cycle) and swing phase (40% of the gait cycle). Although, healthy persons walking is characterized by a repetition of the gait cycle pattern, significant variations could be seen between different gait cycles during patients' walking (see Figure 2)[34]. Therefore, in this study, the gait cycle is analyzed to classify patients and healthy persons. To extract the gait cycle pattern, 8 sensors are placed in each shoe sole to record vertical Ground Reaction Force (vGRF) during walking (see Figure 4). Afterward, to verify and fine-tune the function of the proposed model, some clinical features are extracted from the recorded vGRF. These high-level clinical features are introduced in Table 3.1. To reduce the dimension of input variables and considering the correlations among features obtained from either left or right foot, here we average values related to both feet and construct one variable for each foot. The final clinical features are introduced in Table 2

Some preprocessing is applied on the obtained vGRF data. First, following [35], to avoid outliers resulted from performing round trip along a walkaway, the recorded gait data during the turn-around phase were removed. Moreover, first and last 20s are removed to eliminate the effects of starting and stopping movement. In addition, a 10-point median filter is applied to remove some fluctuations which can cause non-zero vGRF values during the swing phases. Figure 5 shows the effect of applying the preprocessing on recorded vGRF signals of a subject.

To have a common range of definition, considering different range for different features, we normalize all features to range [0,1].

3.2 Interval Type-2 Fuzzy Neural Network

The general architecture of the proposed interval type-2 fuzzy neural network (IT2FNN) is shown in Figure 6. The inputs to this network are extracted features explained in section 3.1, and its output is the degree in range [-1,1] indicating how much the subject is suspicious to have Parkinson's Disorder. This IT2FNN is built upon the Mamdani Fuzzy Inference System [40], using Minimum function as the t-norm operator. Therefore, it reduces the restriction on firing fuzzy rules. Furthermore, it is assumed that the fuzzy membership functions are Gaussian with uncertain width. Indeed, based on the proposed learning method (explained in section 3.3) the centers of fuzzy sets are extracted but there is no clue for the precise values of their width. To solve this problem, the width of fuzzy sets considered uncertain. This assumption improves the robustness of the model against uncertainty and sensor noisy measurements as

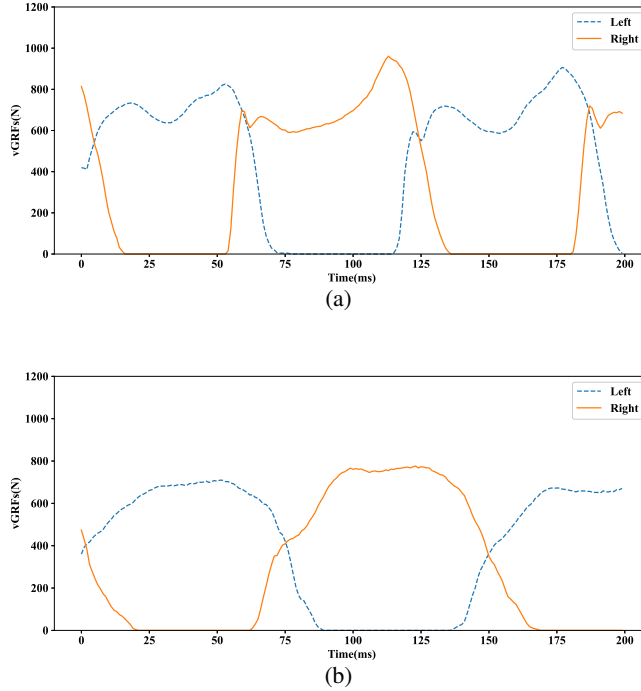


Figure 2: Comparing the gait cycle obtained from vGRF of a healthy subject (a) and a patient suffering from Parkinson's Disease (b).

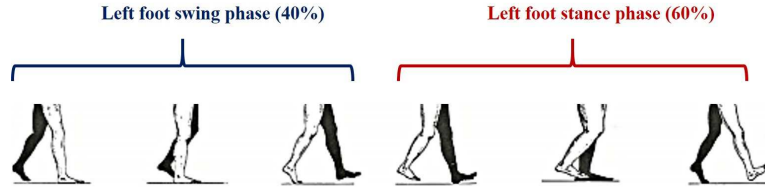


Figure 3: Gait cycle (inspired by [35, 5]).

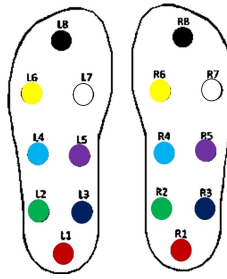


Figure 4: Placement of different sensors under feet (inspired by [35]).

investigated in section 4. For type reduction, the direct BMM method [7, 8, 43] is applied with equal weight parameters [33]. The details of each layer are explained as follows:

1. *Input Layer*: This layer encodes the input variable vector extracted from the gait cycle of the subject. The output of this layer is as follows:

$$X = [x_1, x_2, \dots, x_{10}]^T \quad (1)$$

where, x_1 to x_{10} are extracted features from the gait cycle introduced in Table 2.

2. *Fuzzification Layer*: There are two types of neurons in this layer to encode the interval type-2 fuzzy sets used for defining different fuzzy rules. For i^{th} ($i = 1, 2, \dots, R$) fuzzy rule, the interval type-2 fuzzy membership value of j^{th} ($j = 1, 2, \dots, 10$) input variable is defined as follows:

$$\underline{\mu}_{i,j}(x_j) = e^{-\frac{1}{2} \frac{(x_j - c_{ij})^2}{\underline{\sigma}^2}} \quad (2)$$

$$\overline{\mu}_{i,j}(x_j) = e^{-\frac{1}{2} \frac{(x_j - c_{ij})^2}{\overline{\sigma}^2}} \quad (3)$$

where, $\underline{\mu}_{i,j}$, and $\overline{\mu}_{i,j}(x_j)$ are lower and upper membership functions (LMF and UMF) of j^{th} input variable to the i^{th} fuzzy rule indicating the footprint of uncertainty (FOU), c_{ij} is the center of the defined fuzzy set for j^{th} input variable in the i^{th} fuzzy rule, $\underline{\sigma}$ is the width of lower membership functions, and $\overline{\sigma}$ is the width of upper membership functions.

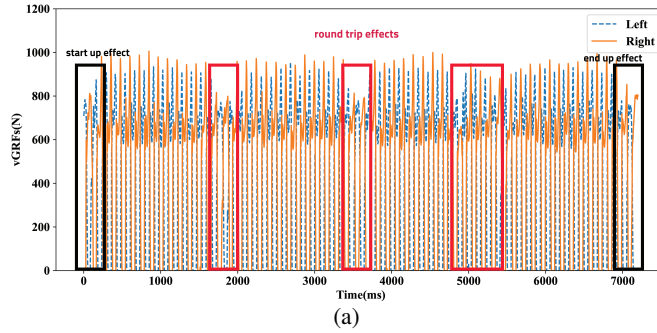
3. *T-Norm Layer*: The neurons of this layer calculate the interval of fuzzy rules' firing strength by applying minimum as the t-norm operator. Indeed, the upper and lower firing strength of each fuzzy rule is computed

Table 1: List of the fourteen extracted features.

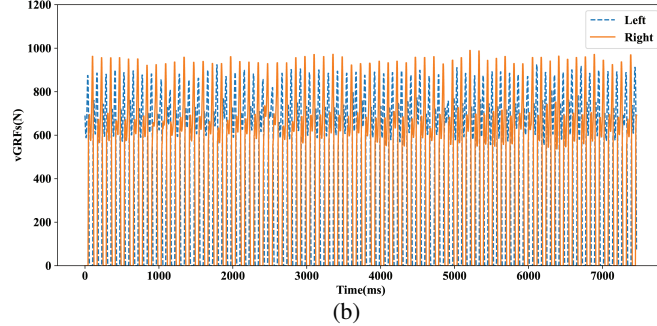
Feature References	Extracted Features	Explanation
z_1	Mean of the Short Swing Time	compare Swing Time between the Right and the Left foot, then distribute it according to the Short Swing Time Criteria (Mean of the Short Swing Time) [63]
z_2	Mean of the Long Swing Time	compare Swing Time between the Right and the Left foot, then distribute it according to the Long Swing Time Criteria (Mean of the Long Swing Time) [63]
z_3	Mean of the Gait Asymmetry	$100 \times \ln(\frac{\text{Short Swing Time}}{\text{Long Swing Time}}) $ (averaged of the Gait Asymmetry) [63]
z_4	Mean in Percentage (%) of the Swing Time of the Left Foot	$100 \times \frac{\text{Duration (s) of Swing Time of the left foot}}{\text{Duration (s) of Stride Time of the left foot}}$ (Mean of the Percentage (%) of the Swing Time of the left foot) [62, 26]
z_5	Mean in Percentage (%) of the Swing Time of the Right Foot	$100 \times \frac{\text{Duration (s) of Swing Time of the right foot}}{\text{Duration (s) of Stride Time of the right foot}}$ (Mean of the Percentage (%) of the Swing Time of the right foot) [62, 26]
z_6	Mean in duration (s) of the Swing Time of the left Foot	Time of the left foot was in the air (Mean of the duration (s) of the Swing Time of the left foot) [28, 62, 19]
z_7	Mean in duration (s) of the Swing Time of the Right Foot	Time of the right foot was in the air (Mean of the duration (s) of the Swing Time of the right foot) [28, 62, 19]
z_8	Coefficients of Variations of the Short Swing Time	$100 \times \frac{\text{Standard Deviation of the Short Swing Time}}{\text{Mean of the Short Swing Time}}$ [63]
z_9	Coefficients of Variations of the Long Swing Time	$100 \times \frac{\text{Standard Deviation of the Long Swing Time}}{\text{Mean of the Long Swing Time}}$ [63]
z_{10}	Coefficients of Variations of the Gait Asymmetry	$100 \times \ln(\frac{\text{Coefficient of Variation of the Short Swing Time}}{\text{Coefficient of Variation of the Long Swing Time}}) $ [63]
z_{11}	Coefficient of Variations in duration (s) of the Swing Time of the Left foot	$100 \times \frac{\text{Standard Deviation in duration (s) of the Swing Time of the left foot}}{\text{Mean in duration (s) of the Swing Time of the left foot}}$ [63]
z_{12}	Coefficient of Variations in duration (s) of the Swing Time of the Right foot	$100 \times \frac{\text{Standard Deviation in duration (s) of the Swing Time of the Right foot}}{\text{Mean in duration (s) of the Swing Time of the Right foot}}$ [63]
z_{13}	Coefficient of Variations in duration (s) of the Stride Time of the Left foot	$100 \times \frac{\text{Standard Deviation in duration (s) of the Stride Time of the left foot}}{\text{Mean in duration (s) of the Stride Time of the left foot}}$ [62]
z_{14}	Coefficient of Variations in duration (s) of the Stride Time of the Right foot	$100 \times \frac{\text{Standard Deviation in duration (s) of the Stride Time of the right foot}}{\text{Mean in duration (s) of the Stride Time of the right foot}}$ [62]

Table 2: Final clinical features based on the initial list presented in Table 3.1.

Feature Symbol	Feature Value
x_1	z_1
x_2	z_2
x_3	z_3
x_4	$\frac{z_4+z_5}{2}$
x_5	$\frac{z_6+z_7}{2}$
x_6	z_8
x_7	z_9
x_8	z_{10}
x_9	$\frac{z_{11}+z_{12}}{2}$
x_{10}	$\frac{z_{13}+z_{14}}{2}$



(a)



(b)

Figure 5: Effect of applying preprocessing on vGRF signals of a subject. (a) before preprocessing, (b) after preprocessing.

based on applying t-norm operator on upper and lower membership values calculated in the previous layer as follows:

$$\underline{\phi}_i = \text{Min}_{j=1}^n \underline{\mu}_{i,j}(x_j) \quad (4)$$

$$\overline{\phi}_i = \text{Min}_{j=1}^n \overline{\mu}_{i,j}(x_j) \quad (5)$$

where $\underline{\phi}_i$ and $\overline{\phi}_i$ are lower and upper firing strength of the i^{th} fuzzy rule.

4. *Aggregation Layer*: Neurons of this layer calculates the boundaries of the network's output $[\underline{y}, \overline{y}]$ receiving the firing strength interval calculated in the T-Norm Layer as follows:

$$\begin{cases} \underline{y} = \sum_{i=1}^R y_i \underline{\phi}_i \\ \overline{y} = \sum_{i=1}^R y_i \overline{\phi}_i \end{cases} \quad (6)$$

where, the consequent part's parameter of i^{th} fuzzy rule shown by y_i is a real value in the range $[-1, 1]$ indicating the degree of being a patient ($y_i = 1$ indicates the patient class and $y_i = -1$ indicated the healthy one).

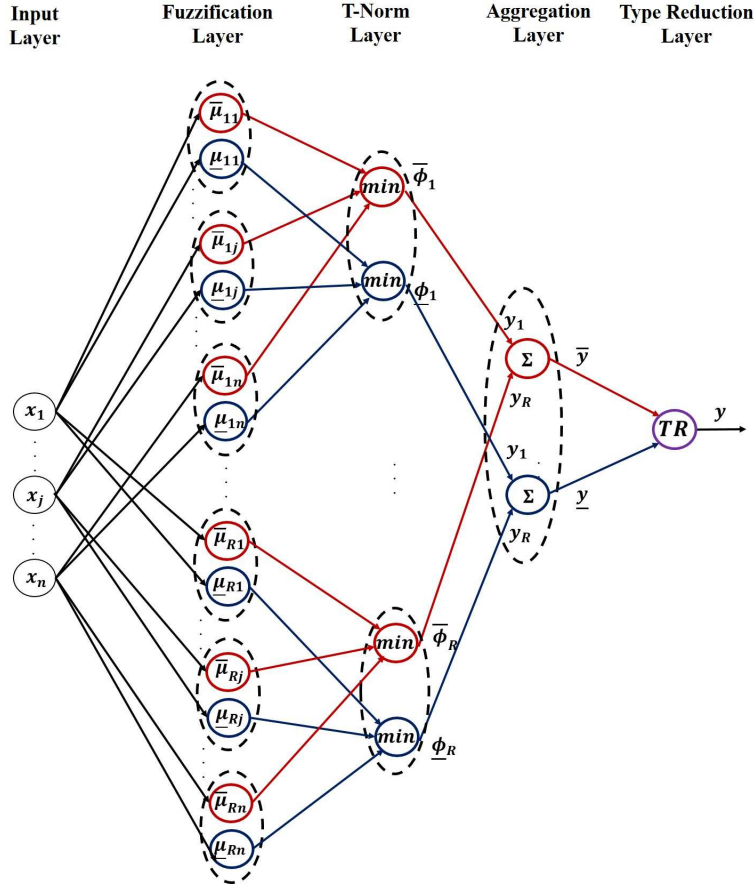


Figure 6: The proposed interval type-2 fuzzy neural network architecture.

5. *Type Reduction Layer*: This layer is composed of one neuron that decides whether the input vector belongs to a patient or a healthy subject. The output neuron calculated the weighted average of fuzzy rules outputs as follows:

$$y = y + \bar{y} \quad (7)$$

if $y > 0$, the final decision would be patient, else the input sample is classified as healthy.

It is worthy to mention that two final layers (aggregation and type-reduction layers) realizes the direct BMM type-reduction and defuzzification with equal weights [7, 8, 33, 43].

This Interval Type-2 Fuzzy Neural Network realizes an Interval Type-2 [38] Mamdani Fuzzy Inference Systems (FIS) [40] and its fuzzy rules can be interpreted in the form of:

Fuzzy Rule i : IF x_1 is $\tilde{A}_{i,1}$ and x_2 is $\tilde{A}_{i,2}$ and ... and x_{10} is $\tilde{A}_{i,10}$ Then y is y_i

where, $\tilde{A}_{i,j}$ ($j = 1, 2, \dots, 10$) is a Gaussian interval type-2 fuzzy set with uncertain width (see Figure 7) defined for i^{th} fuzzy rule and j^{th} variable (x_j in Table 2), y is the output of the FIS, and $y_i \in [-1, 1]$ is the consequent part of i^{th} fuzzy rule. To report the fuzzy rules, it is sufficient to report the extracted centers for all interval type-2 fuzzy sets $\tilde{A}_{i,j}$.

3.3 Learning Algorithm

The introduced network in section 3.2 has two categories of parameters we should determine to classify subjects properly: 1- Fuzzy rules antecedent parts' parameters including the centers and width of fuzzy sets, 2- Fuzzy rules consequent parts' parameters indicating the decision of each fuzzy rule (y_i). We determine these parameters by applying a centroid-based clustering method, like Fuzzy C-Means [6] on training samples as follows:

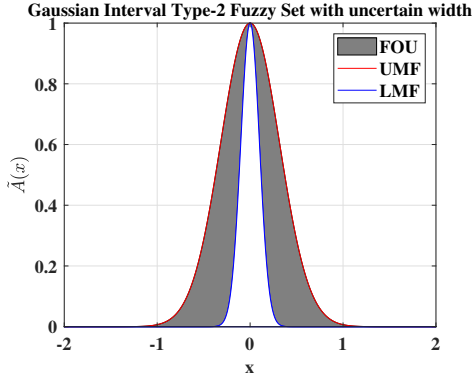


Figure 7: An example of an interval type-2 fuzzy set with uncertain width. UMF: Upper Membership Function, LMF: Lower Membership Function, FOU: Footprint of Uncertainty.

1. Divide the training samples into R clusters. Here, the desired output (label) which is $+1$ for patients and -1 for healthy subjects is considered as an input variable. Therefore, the k^{th} training sample X_k has a vector with 11 dimensions as follows:

$$X_k = [x_{k,1}, x_{k,2}, \dots, x_{k,10}, y_k^*] \quad (8)$$

where $x_{k,j}$ ($j = 1, 2, \dots, 10$) are values of input variables for k^{th} sample and y_k^* is its desired output value. Using the output value along with input variables causes that the clustering approach considers the classes of training instances in composing clusters.

2. After clustering, i^{th} ($i = 1, 2, \dots, R$) cluster has a center vector V_i representing that cluster. These centers are used as the centers of fuzzy sets composing each fuzzy rule.
3. To determine the consequent part parameters y_i for i^{th} fuzzy rule, a weighted average of desired outputs of training samples belongs to the i^{th} cluster is calculated as follows:

$$y_i = \frac{\sum_{k=1}^N u_{i,k}^m \cdot y_k^*}{\sum_{k=1}^N u_{i,k}^m} \quad (9)$$

where y_k^* is desired output value for k^{th} training sample, $u_{i,k}$ is the fuzzy membership value of k^{th} training sample to the i^{th} cluster calculated during the clustering, N is the number of training samples, and $m > 1$ is the fuzzy partition exponent for controlling the degree of fuzzy overlap in FCM algorithm.

4. To determine the fuzzy sets width, considering the uncertainty we assume that the width belongs to the range $[\sigma_1, \sigma_2]$ where σ_1 and σ_2 are two constant values lower than 1. Therefore, σ_1 is considered as the width of the lower membership functions, and σ_2 is considered as the width of the upper membership function as follows:

$$\frac{\sigma}{\bar{\sigma}} = \frac{\sigma_1}{\sigma_2} \quad (10)$$

The proposed learning algorithm is summarized in Algorithm 1.

3.4 Complementary Online Learning

The proposed learning method is a kind of batch learning approach based on clustering all samples which assumes that all training instances are available at once. This is partially true that we should have training examples for training the fuzzy neural network at first. However, it is possible that more studies may gather more examples in the future. Therefore, to avoid learning the network from scratch, here we propose a complementary learning approach to able the network handing the new training instances whenever is necessary. The proposed complementary online learning approach is based on investigating the amount of current fuzzy rules' coverage encountering a new instance [55, 53]. If the coverage of existing fuzzy rules is not sufficiently encountering a new example, a new fuzzy rule is added to the Fuzzy Neural Network to cover an area consisting of this new sample and future similar instances. Indeed, if the sum of fuzzy rules firing strength is lower than a predefined threshold, a new fuzzy rule based on this new sample is added to the network. The center of this newly added fuzzy rule would be the arrived new instance and the width would be lower than the previous fuzzy rules to decrease the conflict with previous fuzzy rules and only cover the region

Algorithm 1: Learning algorithm

Inputs:
 training samples X along with their desired output values Y^*
 number of rules (R), number of samples (N)
 range of fuzzy sets width (σ_1, σ_2), fuzzy overlap degree m

Outputs:
 center of fuzzy sets ($c_{i,j}$), width of lower and upper membership functions ($\underline{\sigma}$ & $\bar{\sigma}$)
 the consequent parts' parameters y_i
 $X_{aug} \leftarrow [X, Y^*]$;
 Calculates the cluster centers V and membership matrix u based on FCM:
 $[V, u] \leftarrow FCM(X_{aug}, m, R)$;

```

for  $i \leftarrow 1$  to  $R$  do
    for  $j \leftarrow 1$  to  $10$  do
         $| c_{i,j} \leftarrow V_{i,j} ;$ 
    end
     $y_i \leftarrow 0 ;$ 
     $s \leftarrow 0 ;$ 
    for  $k \leftarrow 1$  to  $N$  do
         $| y_i \leftarrow y_i + u_{i,k}^m * Y_k^* ;$ 
         $| s \leftarrow s + u_{i,k}^m ;$ 
    end
     $y_i \leftarrow y_i / s ;$ 
end
 $\underline{\sigma} \leftarrow \sigma_1 ;$ 
 $\bar{\sigma} \leftarrow \sigma_2 ;$ 

```

Algorithm 2: Complementary Online Learning Algorithm

Inputs:
 New training sample x_{new} along with its desired output values y_{new}^*
 number, centers, width and consequent parameters of existing rules ($R, c, \bar{\sigma}, \underline{\sigma}, y$)
 threshold of coverage θ_c
 coefficient ϵ to justify the width of added fuzzy rules

Outputs:
 updated center of fuzzy sets ($c_{i,j}$), width of lower and upper membership functions ($\underline{\sigma}$ & $\bar{\sigma}$)
 updated consequent parts' parameters y_i
 compute the decision of fuzzy neural network for x_{new} as \hat{y}_{new}

```

if  $\hat{y}_{new} \neq y_{new}^*$  then
     $S \leftarrow 0 ;$ 
    for  $i \leftarrow 1$  to  $R$  do
         $| S \leftarrow S + \phi_i(x_{new}) ;$ 
    end
    if  $S < \theta_c$  then
         $| R \leftarrow R + 1 ;$ 
        for  $j \leftarrow 1$  to  $n$  do
             $| c_{R,j} \leftarrow x_{new,j} ;$ 
        end
         $| y_R \leftarrow y_{new}^* ;$ 
         $| \bar{\sigma}_R \leftarrow \epsilon \times \bar{\sigma} ;$ 
         $| \underline{\sigma}_R \leftarrow \epsilon \times \underline{\sigma} ;$ 
    end
end

```

with a low amount of coverage. The consequent part of this new fuzzy rule is the desired output of the newly arrived instance. Figure 8 shows an illustrative example of adding a new fuzzy rule in a two-dimensional space and Algorithm 2 summarizes this complementary online learning. The paradigm of complementary online learning is shown in Figure 9.

4 Experimental Results

In this section, the performance of the proposed method is evaluated and compared to some previous methods. First, the utilized data is explained. Next, the evaluation metrics used for evaluating the performance of the method are introduced. Afterward, the performance of the proposed paradigm is compared to some supervised and unsupervised machine learning approaches applied to similar data in the literature. Next, the effectiveness of the proposed complementary online learning method is investigated. To investigate the effectiveness of using Interval Type-2 Fuzzy Logic, the performance of the proposed method is compared with the performance of a similar type-1 fuzzy neural network encountering noisy data. Afterward, the final fuzzy sets and rules extracted by the proposed method are reported. These reported fuzzy rules can be used by experts to: 1- evaluate the extracted fuzzy rules and fine-tune them, and 2- apply them to classify patients and healthy persons.

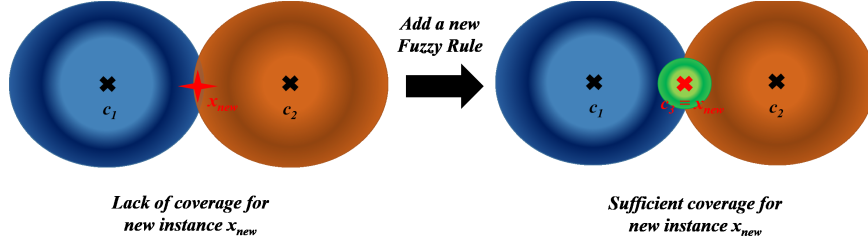


Figure 8: An illustrative example of adding a new fuzzy rule in a two-dimensional input space. First, the input vector x_{new} is analyzed by two existing fuzzy rules with centers c_1 and c_2 . The total coverage for the sample x_{new} is lower than a predefined threshold θ_c . Consequently, a new fuzzy rule, which its center is x_{new} , has been added.

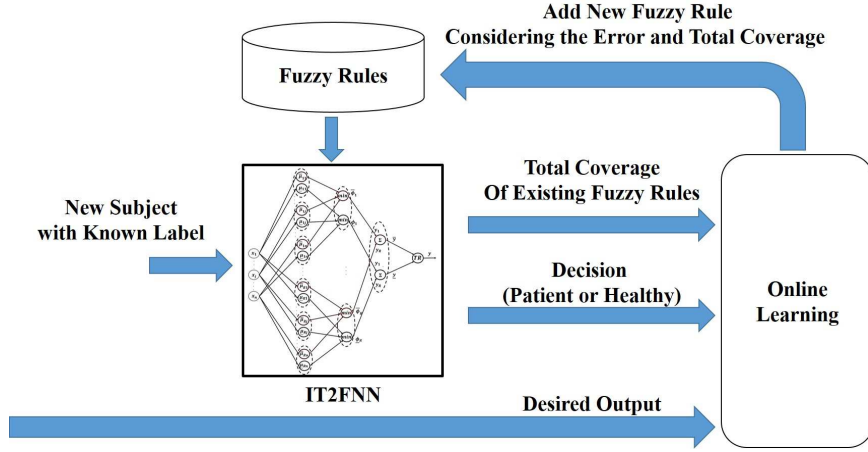


Figure 9: The paradigm of online learning.

4.1 Data

We utilized the gait cycle data provided by PhysioNet¹. This data aggregates three similar sub-datasets obtained in different experimental studies from different subjects [20, 62, 27]. The dataset includes vGRF obtained from 16 sensors placed under feet of control and patient subjects (8 per foot) as shown in Fig. 4. Totally, the data were recorded from 93 patients with PD and 72 healthy control subjects. The vertical ground reaction force recorded of subjects as they walked at their usual, self-selected pace for approximately 2 minutes on level ground. Features are extracted from two sequences indicating the average vGRF of each foot. The details of each dataset are outlined in Table 3.

4.2 Evaluation Metrics

To evaluate the performance of the proposed method, the usual metrics utilized in the classification tasks are used. One of the most popular metrics in classification tasks is "Accuracy" that shows the average performance of the method to properly classify instances and is defined as follows:

$$Accuracy = \frac{TP + TN}{TP + TN + FP + FN} \quad (11)$$

where TP ("True Positive") is the number of instances that belongs to the positive class (here PD patient) classified correctly, TN (True Negative) is the number of instances belongs to the negative class (here healthy persons) classified correctly, FP (False Positive) is the number of instances belongs to the negative class but classified wrongly, and finally, FN (False Negative) is the number of instances belonging to the positive class but classified wrongly.

In some applications like medical diagnosis, it is very important to avoid False Positives and also detect the patients correctly. Detecting a healthy person as a patient would lead to extra costs (e.g. additional experiments) and also disappointment for the person and his/her family. On the other hand, if the system detects a patient as a healthy person,

¹<https://physionet.org/content/gaitpdb/1.0.0/>

Table 3: Information of different datasets used for evaluation of the method (CO: Healthy Control Subject, PD: Patients with Parkinson's Disease).

Data	Subjects	Total subjects	Female	Male
Ga [62]	PD	29	9	20
	CO	18	8	10
Si [20]	PD	35	13	22
	CO	29	11	18
Ju [27]	PD	29	13	16
	CO	25	14	12

Table 4: Comparison of the performance of the proposed method with other approaches in the case of the Yoge et al. (Ga) sub-datasets.

Performance Metric	Propose Method	KNN [35]	CART [35]	RF [35]	NB [35]	SVM [35]	K-Means [35]	GMM [35]
Accuracy	92.92	86.05	83.72	86.05	74.42	86.05	63.72	64.77
Precision	92.40	84.89	82.86	85.07	74.73	84.90	64.34	62.63
Recall	97.33	86.34	81.94	85.07	76.45	85.71	65.31	62.91
F1 Score	94.80	85.61	82.40	85.07	75.58	85.30	64.82	62.77

it would be dangerous for his/her health. Therefore, to have a more precise evaluation, the following metrics are also utilized:

$$Precision = \frac{TP}{TP + FP} \quad (12)$$

$$Recall = \frac{TP}{TP + FN} \quad (13)$$

$$F_1 = \frac{2.Precision.Recall}{Precision + Recall} \quad (14)$$

where, Precision evaluates the False Positive rate, Recall evaluates the ability of the method to classify patients correctly, and F_1 score is a combination of Precision and Recall.

4.3 Results

Tables 4 to 6 evaluate the performance of the method based on different criteria in different datasets introduced in Table 3. The performance of the proposed method is compared with the performance of the methods used similar clinical features in [35]. Following [35], each sub-dataset is divided into training and testing sets according to the leave-one-out cross-validation procedure.

According to the results reported in Tables 4 to 6. the proposed method outperforms all other supervised and supervised machine learning approaches trained with similar features in sub-dataset Ga, and Si. In sub-dataset Ju, two supervised machine learning approaches KNN and SVM have better Accuracy, the proposed method has a better Precision, Recall, and F1 Score. Indeed, the proposed method has a lower False Negative rate which is very important in a clinical application. Moreover, the proposed method is an interpretable approach, and experts can use the extracted fuzzy rules or fine-tune them. Tables 7 to 9 show the true positive and true negative rates of the proposed method and compare its performance with other methods. The proposed method performs worse than KNN in Ju sub-dataset in detecting healthy control subjects. The reason could be low coverage of healthy input space by the gathered data in Ju sub-dataset. Therefore, there are not sufficient healthy instances to cover the input space efficiently. Subsequently, the KNN approach that saves all instances and votes in a neighborhood around the test example performs better than the proposed method in this sub-dataset.

For parameter setting, we should determine the number of fuzzy rules and the width of fuzzy sets. The width of fuzzy sets are considered in the range $[0.01, 0.1]$. Indeed, it is assumed that each fuzzy set could be very uncertain ($\sigma = 0.1$) or close to a precise value ($\sigma = 0.01$) for decision making. To determine the number of fuzzy rules, the performance of the method is evaluated for a different number of fuzzy rules for 10 independent runs and then we have calculated the mean and the standard deviation (STD) of the F1 score regarding different number of fuzzy rules. Afterward, the lowest number of fuzzy rules with higher mean and lower STD is chosen for each dataset (see Figure 10). Based on Figure 10, the chosen number of fuzzy rules are listed in Table 10.

Table 5: Comparison of the performance of the proposed method with other approaches in the case of the Hausdorff et al. (Ju) sub-datasets.

Performance Metric	Propose Method	KNN [35]	CART [35]	RF [35]	NB [35]	SVM [35]	K-Means [35]	GMM [35]
Accuracy	85.83	90.91	84.30	87.60	77.69	90.08	55.12	65.12
Precision	88.89	85.35	82.34	89.41	70.64	89.31	52.58	57.95
Recall	93.62	88.35	64.96	71.48	78.54	78.96	53.91	61.29
F1 Score	91.19	86.83	72.62	79.45	74.38	83.82	53.24	59.57

Table 6: Comparison of the performance of the proposed method with other approaches in the case of the Frenkel-Toledo et al. (Si) sub-datasets.

Performance Metric	Propose Method	KNN [35]	CART [35]	RF [35]	NB [35]	SVM [35]	K-Means [35]	GMM [35]
Accuracy	83.33	81.25	79.69	82.81	79.69	82.81	57.19	65.31
Precision	85.71	81.43	79.56	83.10	79.69	82.81	61.07	64.95
Recall	85.71	81.67	79.36	82.22	79.95	83.10	59.23	64.62
F1 Score	85.71	81.55	79.46	82.65	79.82	82.96	60.14	64.78

4.4 Effectiveness of the Online Learning

To evaluate the effectiveness of the proposed complementary online learning, we assume that only one sub-set is available as the initial training dataset. After learning the Interval Type-2 Fuzzy Neural Network and extracting the fuzzy rules, another sub-dataset is added as new training samples. We assume that the sub-dataset Ga [62] is available and after training, the samples of sub-dataset Ju will be added. Table 11 compares the performance of the method before and after adding new instances. It is shown that the number of fuzzy rules is increased and the performance of the method is improved for all sub-datasets. The threshold for investigating the amount of fuzzy rules’ coverage is set 0.1. The ϵ parameter in Algorithm 2 is set at 1.

4.5 Effectiveness of Interval Type-2 Fuzzy System against Noisy Data

To investigate the effectiveness of the proposed Interval Type-2 Fuzzy system against noisy data, its performance is compared with a type-1 fuzzy neural network applying on noisy test samples. In this experiment, all samples of sub-datasets Ga, Ju, and Si are gathered together to form one dataset. Next, it is divided into training and testing sets according to the leave-one-out cross-validation procedure. We add a Gaussian noise with different width values 0.1 and 0.3 to the test samples. The number of fuzzy rules is considered as 10. Table 12 shows the effectiveness of the proposed Interval Type-2 Fuzzy Neural Network comparing its performance with a Type-1 Fuzzy Neural Network.

4.6 Final Extracted Fuzzy Rules

In this part, whole available samples are fed to the Interval Type-2 Fuzzy Neural Network to extract final fuzzy rules based on the currently available data. The number of fuzzy rules is set to 9. The performance of the method is summarized in Table 13. Figure 11 shows extracted fuzzy sets for all features. It is obvious that based on the available data and importance of different ranges of values, the density of defined fuzzy sets in different regions of different features is various. Figure 12 shows the extracted fuzzy rules. Each row indicates a fuzzy rule and each column indicates a feature. The center of fuzzy sets used for constructing each rule is shown in each cell and the color of each cell represents the sense of the linguistic variable (higher values are near to red and lower values are close to white). The

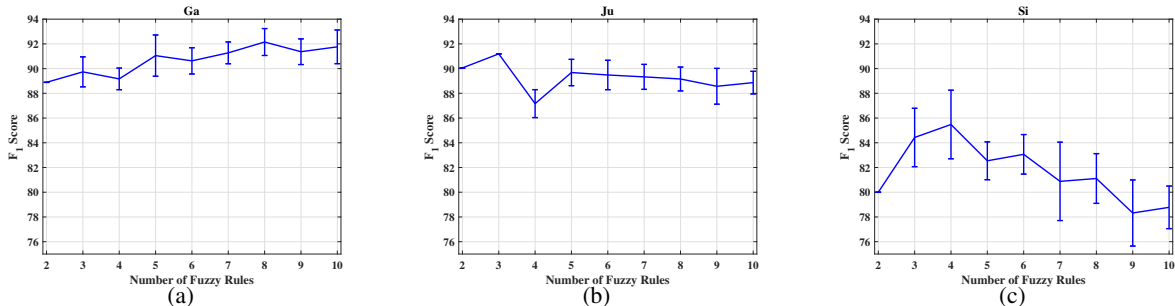


Figure 10: Mean and standard deviation of the performance of the method regarding different number of fuzzy rules.

Table 7: Global confusion matrix obtained using the different classifiers in the case of the Yogev et al. (Ga) sub-dataset (H: Healthy, P: Patient).

		Obtained Classes																			
		Proposed Method				KNN				CART				RF		NB		SVM		K-Means	
		H	P	H	P	H	P	H	P	H	P	H	P	H	P	H	P	H	P	H	P
True Classes	H	84.21	15.79	87.50	12.50	75.00	25.00	81.25	18.75	84.38	15.62	84.38	15.62	71.53	28.47	55.63	44.37				
	P	2.67	97.33	14.81	85.19	11.11	88.89	11.11	88.89	31.48	68.52	12.96	87.04	40.91	59.09	29.81	70.19				

Table 8: Global confusion matrix obtained using the different classifiers in the case of the Hausdorff et al. (Ju) sub-dataset (H: Healthy, P: Patient).

		Obtained Classes																			
		Method				KNN				CART				RF		NB		SVM		K-Means	
		H	P	H	P	H	P	H	P	H	P	H	P	H	P	H	P	H	P	H	P
True Classes	H	57.69	42.31	84.00	16.00	32.00	68.00	44.00	56.00	80.00	20.00	60.00	40.00	51.84	48.16	54.76	45.24				
	P	6.38	93.62	7.29	92.71	2.08	97.92	1.04	98.96	22.92	77.08	2.08	97.92	44.02	55.98	32.19	67.81				

last column shows the consequent parts' parameters which is the proposed label of each fuzzy rule ('+1' for patients (colored red) and '-1' for healthy subjects (colored blue)).

5 Conclusions

In this paper, a classifier using an interval type-2 fuzzy neural network is proposed to diagnose patients suffering from Parkinson's Disease (PD). The proposed method analyzes the gait cycle of subjects recorded in the form of vertical Ground Reaction Force (vGRF) signals. To have an interpretable system, 10 clinical features are extracted from the vGRF signal. To overcome the uncertainty and sensor noisy measurements, the fuzzy neural network is built upon interval type-2 fuzzy logic.

To extract fuzzy rules, two paradigms are presented. First, using the available training dataset, initial interpretable fuzzy rules are extracted. To able system learning from new instances, an online learning approach is proposed. This complementary online learning investigates the performance and coverage of the current rule base. In the case of wrong classification and low coverage, a new fuzzy rule is added to the rule base.

The performance of the proposed method is evaluated on three datasets obtained from different subjects ([62, 20, 27]) and compared with other supervised and unsupervised machine learning approaches using similar clinical features. Moreover, the performance of the model in the presence of noise is evaluated and compared with a T1 fuzzy neural network. The effectiveness of online learning is investigated by adding new training instances after finishing batch learning. This experiment shows an obvious improvement in the network's performance after applying the proposed online learning. Finally, the extracted fuzzy sets of different features are reported.

Using meta-heuristic optimization methods like Evolutionary Algorithms and Swarm Intelligence method for fine-tuning rules' parameters is proposed as the future study.

Table 9: Global confusion matrix obtained using the different classifiers in the case of the Frenkel-Toledo et al. (Si) sub-dataset (H: Healthy, P: Patient).

		Obtained Classes															
		Proposed Method		KNN		CART		RF		NB		SVM		K-Means		GMM	
True Classes		H	P	H	P	H	P	H	P	H	P	H	P	H	P	H	P
	H	80.00	20.00	86.21	13.79	75.86	24.14	75.86	24.14	82.76	17.24	86.21	13.79	80.97	19.03	57.24	42.76
	P	14.29	85.71	22.86	77.14	17.14	82.86	11.43	88.57	22.86	77.14	20.00	80.00	62.51	37.49	28.00	72.00

Table 10: Chosen number of fuzzy rules based on studies reported in Figure 10.

	Data	Ga	Ju	Si
Number of Fuzzy Rules	8	3	4	

Table 11: Evaluating the effectiveness of online learning. The initial available training dataset includes Ga and after training, Ju is added

State	Number of Fuzzy Rules	Data	Accuracy	Precision	Recall	F1 Score
Trained using Ga	8	Ga	92.92	94.66	94.66	94.66
		Ju	75.00	77.78	80.00	78.87
		Si	81.66	90.00	86.17	88.04
Added Ju	10	Ga	93.80	93.59	97.33	95.42
		Ju	83.33	80.48	94.28	86.84
		Si	87.50	88.34	96.81	92.38

Table 12: Evaluating the effectiveness of Interval Type-2 Fuzzy Neural Network against noisy data.

Noise	Number of Fuzzy Rules	Data	Method	Accuracy	Precision	Recall	F1 Score
0.1	10	Ga	IT2	91.96	93.42	94.66	94.04
			T1	89.28	89.87	94.66	92.20
		Ju	IT2	89.74	91.83	95.74	93.75
			T1	86.32	88.23	95.74	91.83
		Si	IT2	81.25	78.04	91.42	84.21
			T1	81.25	76.74	94.28	84.61
			IT2	83.03	87.83	86.66	87.24
	10	Ga	T1	84.82	88.15	89.33	88.74
			IT2	83.76	92.13	87.23	89.61
		Ju	T1	80.34	87.36	88.29	87.83
			IT2	76.56	79.41	77.14	78.26
			T1	67.18	69.44	71.42	70.42

Table 13: Final performance of the proposed method trained using all available data

Accuracy	Precision	Recall	F1 Score
88.74	89.41	95.10	92.16

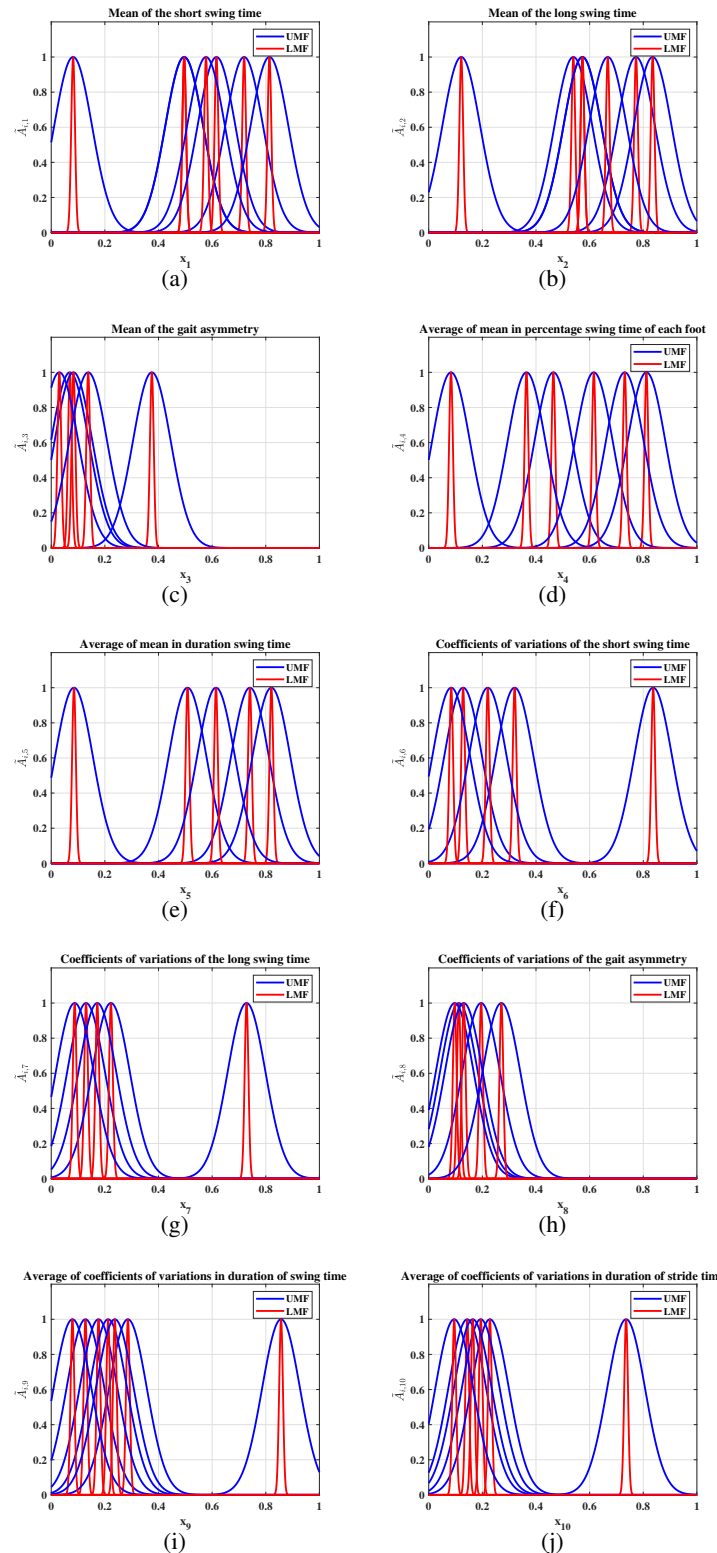


Figure 11: Extracted Interval Type-2 fuzzy sets for different features.

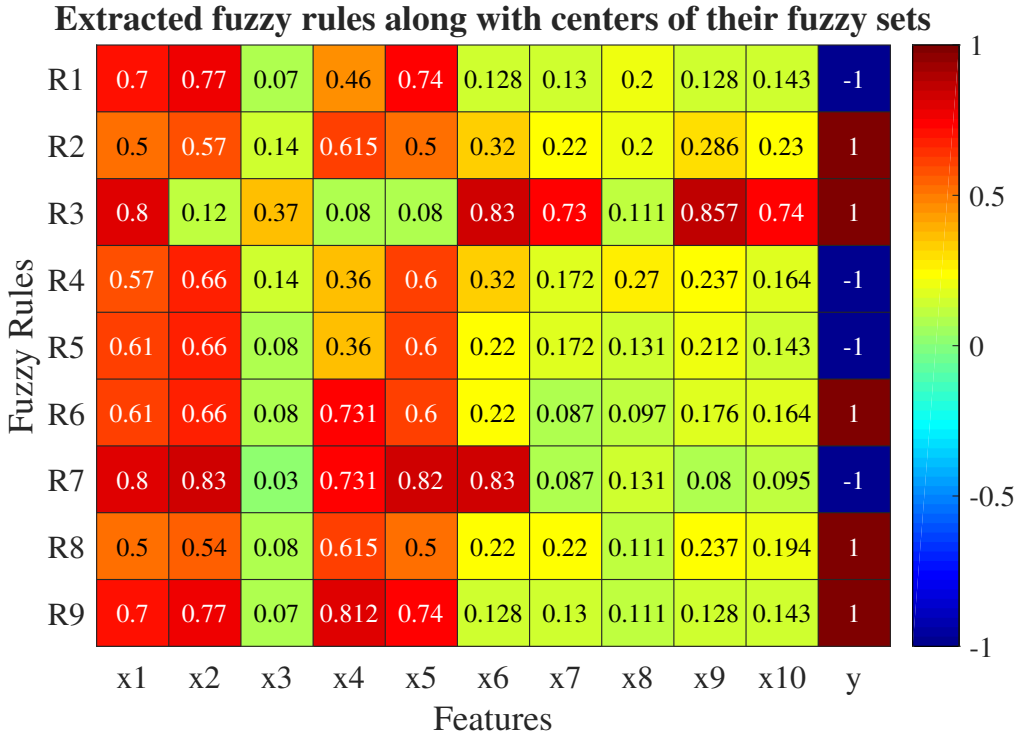


Figure 12: Extracted fuzzy rules. Each row indicates a fuzzy rule (R_1 to R_9) and each column except the last indicates a feature (x_1 to x_{10}). The last column presents each fuzzy rule's output value as the consequent part's parameter ('+1' for patients (colored red) and '-1' for healthy subjects (colored blue)). The center of fuzzy sets used for constructing each rule is shown in each cell and the color of each cell represents the sense of the linguistic variable (higher values are near to red and lower values are close to white).

References

- [1] I Antonio-Rubio, CJ Madrid-Navarro, E Salazar-López, MJ Pérez-Navarro, C Sáez-Zea, E Gómez-Milán, A Mínguez-Castellanos, and F Escamilla-Sevilla. Abnormal thermography in parkinson's disease. *Parkinsonism & related disorders*, 21(8):852–857, 2015.
- [2] Karalikkadan Ashhar, Cheong Boon Soh, and Keng He Kong. A wearable ultrasonic sensor network for analysis of bilateral gait symmetry. In *2017 39th Annual International Conference of the IEEE Engineering in Medicine and Biology Society (EMBC)*, pages 4455–4458. IEEE, 2017.
- [3] Freddie Åström and Rasit Koker. A parallel neural network approach to prediction of parkinson's disease. *Expert systems with applications*, 38(10):12470–12474, 2011.
- [4] Chiara Baiano, Paolo Barone, Luigi Trojano, and Gabriella Santangelo. Prevalence and clinical aspects of mild cognitive impairment in parkinson's disease: A meta-analysis. *Movement Disorders*, 35(1):45–54, 2020.
- [5] H Bätzner, M Oster, M Daffertshofer, and M Hennerici. Assessment of gait in subcortical vascular encephalopathy by computerized analysis: a cross-sectional and longitudinal study. *Journal of neurology*, 247(11):841–849, 2000.
- [6] James C Bezdek, Robert Ehrlich, and William Full. Fcm: The fuzzy c-means clustering algorithm. *Computers & geosciences*, 10(2-3):191–203, 1984.
- [7] Mohammad Biglarbegian, William W. Melek, and Jerry M. Mendel. Design of novel interval type-2 fuzzy controllers for modular and reconfigurable robots: Theory and experiments. *IEEE Transactions on Industrial Electronics*, 58(4):1371–1384, 2011.
- [8] Mohammad Biglarbegian, William W. Melek, and Jerry M. Mendel. On the robustness of type-1 and interval type-2 fuzzy logic systems in modeling. *Information Sciences*, 181(7):1325–1347, 2011.
- [9] Chien-Wen Cho, Wen-Hung Chao, Sheng-Huang Lin, and You-Yin Chen. A vision-based analysis system for gait recognition in patients with parkinson's disease. *Expert Systems with applications*, 36(3):7033–7039, 2009.
- [10] Mohammad Reza Daliri. Automatic diagnosis of neuro-degenerative diseases using gait dynamics. *Measurement*, 45(7):1729–1734, 2012.
- [11] Resul Das. A comparison of multiple classification methods for diagnosis of parkinson disease. *Expert Systems with Applications*, 37(2):1568–1572, 2010.
- [12] J. de Jesus Rubio. SOFMLS: Online self-organizing fuzzy modified least-squares network. *IEEE Trans. Fuzzy Syst.*, 17(6):1296–1309, 2009.
- [13] Ben Dror, Eilon Yanai, Alex Frid, Nimrod Peleg, Nadav Goldenthal, Ilana Schlesinger, Hagit Hel-Or, and Shmuel Raz. Automatic assessment of parkinson's disease from natural hands movements using 3d depth sensor. In *2014 IEEE 28th Convention of Electrical & Electronics Engineers in Israel (IEEEI)*, pages 1–5. IEEE, 2014.
- [14] Maria Dyshel, David Arkadir, Hagai Bergman, and Daphna Weinshall. Quantifying levodopa-induced dyskinesia using depth camera. In *Proceedings of the IEEE International Conference on Computer Vision Workshops*, pages 119–126, 2015.
- [15] Mohammad Mehdi Ebadzadeh and Armin Salimi-Badr. CFNN: correlated fuzzy neural network. *Neurocomputing*, 148:430–444, 2015.
- [16] Mohammad Mehdi Ebadzadeh and Armin Salimi-Badr. IC-FNN: a novel fuzzy neural network with interpretable, intuitive, and correlated-contours fuzzy rules for function approximation. *IEEE Trans. Fuzzy Syst.*, 26(3):1288–1302, 2018.
- [17] Seyed-Mohammad Fereshtehnejad, Azadeh Shafeesabet, Mahdiyeh Shafeesabet, Gholam Ali Shahidi, Ahmad Delbari, and Johan Lökk. Mortality in iranian patients with parkinson's disease: Cumulative impact of cardiovascular comorbidities as one major risk factor. *Parkinson's Disease*, 2015, 2015.
- [18] KB Foreman, C Wisted, O Addison, RL Marcus, PC LaStayo, and LE Dibble. Improved dynamic postural task performance without improvements in postural responses: the blessing and the curse of dopamine replacement. *Parkinson's Disease*, 2012, 2012.
- [19] Silvi Frenkel-Toledo, Nir Giladi, Chava Peretz, Talia Herman, Leor Gruendlinger, and Jeffrey M Hausdorff. Effect of gait speed on gait rhythmicity in parkinson's disease: variability of stride time and swing time respond differently. *Journal of neuroengineering and rehabilitation*, 2(1):1–7, 2005.
- [20] Silvi Frenkel-Toledo, Nir Giladi, Chava Peretz, Talia Herman, Leor Gruendlinger, and Jeffrey M Hausdorff. Treadmill walking as an external pacemaker to improve gait rhythm and stability in parkinson's disease. *Movement disorders: official journal of the Movement Disorder Society*, 20(9):1109–1114, 2005.

- [21] Brook Galna, Gillian Barry, Dan Jackson, Dadirayi Mhiripiri, Patrick Olivier, and Lynn Rochester. Accuracy of the microsoft kinect sensor for measuring movement in people with parkinson's disease. *Gait & posture*, 39(4):1062–1068, 2014.
- [22] J.E. Hall. *Guyton and Hall Textbook of Medical Physiology*. Guyton Physiology. Elsevier Health Sciences, 2010.
- [23] Brian Harel, Michael Cannizzaro, and Peter J Snyder. Variability in fundamental frequency during speech in prodromal and incipient parkinson's disease: A longitudinal case study. *Brain and cognition*, 56(1):24–29, 2004.
- [24] Muthusamy Hariharan, Kemal Polat, and Ravindran Sindhu. A new hybrid intelligent system for accurate detection of parkinson's disease. *Computer methods and programs in biomedicine*, 113(3):904–913, 2014.
- [25] Lena Hartelius and Per Svensson. Speech and swallowing symptoms associated with parkinson's disease and multiple sclerosis: a survey. *Folia phoniatrica et logopaedica*, 46(1):9–17, 1994.
- [26] Jeffrey M Hausdorff, Merit E Cudkowicz, Renée Firtion, Jeanne Y Wei, and Ary L Goldberger. Gait variability and basal ganglia disorders: stride-to-stride variations of gait cycle timing in parkinson's disease and huntington's disease. *Movement disorders*, 13(3):428–437, 1998.
- [27] Jeffrey M Hausdorff, Justine Lowenthal, Talia Herman, Leor Gruendlinger, Chava Peretz, and Nir Giladi. Rhythmic auditory stimulation modulates gait variability in parkinson's disease. *European Journal of Neuroscience*, 26(8):2369–2375, 2007.
- [28] Jeffrey M Hausdorff, Dean A Rios, and Helen K Edelberg. Gait variability and fall risk in community-living older adults: a 1-year prospective study. *Archives of physical medicine and rehabilitation*, 82(8):1050–1056, 2001.
- [29] Minna Hong, Joel S Perlmutter, and Gammon M Earhart. A kinematic and electromyographic analysis of turning in people with parkinson disease. *Neurorehabilitation and neural repair*, 23(2):166–176, 2009.
- [30] J.-S.R. Jang. ANFIS: adaptive-network-based fuzzy inference system. *IEEE Trans. Syst., Man, Cybern.*, 23(3):665–685, 1993.
- [31] Hyo-Seon Jeon, Jonghee Han, Won-Jin Yi, BeomSeok Jeon, and Kwang Suk Park. Classification of parkinson gait and normal gait using spatial-temporal image of plantar pressure. In *2008 30th Annual International Conference of the IEEE Engineering in Medicine and Biology Society*, pages 4672–4675. IEEE, 2008.
- [32] Deepak Joshi, Aayushi Khajuria, and Pradeep Joshi. An automatic non-invasive method for parkinson's disease classification. *Computer methods and programs in biomedicine*, 145:135–145, 2017.
- [33] Mojtaba Ahmadieh Khanesar and Jerry M. Mendel. Maclaurin series expansion complexity-reduced center of sets type-reduction + defuzzification for interval type-2 fuzzy systems. In *2016 IEEE International Conference on Fuzzy Systems (FUZZ-IEEE)*, pages 1224–1231, 2016.
- [34] Nicolas Khoury, Ferhat Attal, Yacine Amirat, Abdelghani Chibani, and Samer Mohammed. Cdtw-based classification for parkinson's disease diagnosis. In *ESANN*, 2018.
- [35] Nicolas Khoury, Ferhat Attal, Yacine Amirat, Latifa Oukhellou, and Samer Mohammed. Data-driven based approach to aid parkinson's disease diagnosis. *Sensors*, 19(2):242, 2019.
- [36] Mark L Latash, Alexander S Aruin, Ida Neyman, and John J Nicholas. Anticipatory postural adjustments during self inflicted and predictable perturbations in parkinson's disease. *Journal of Neurology, Neurosurgery & Psychiatry*, 58(3):326–334, 1995.
- [37] Sang-Hong Lee and Joon S Lim. Parkinson's disease classification using gait characteristics and wavelet-based feature extraction. *Expert Systems with Applications*, 39(8):7338–7344, 2012.
- [38] Qilian Liang and Jerry M Mendel. Interval type-2 fuzzy logic systems: theory and design. *IEEE Transactions on Fuzzy systems*, 8(5):535–550, 2000.
- [39] Irene Litvan, Jennifer G Goldman, Alexander I Tröster, Ben A Schmand, Daniel Weintraub, Ronald C Petersen, Brit Mollenhauer, Charles H Adler, Karen Marder, Caroline H Williams-Gray, et al. Diagnostic criteria for mild cognitive impairment in parkinson's disease: Movement disorder society task force guidelines. *Movement disorders*, 27(3):349–356, 2012.
- [40] Ebrahim H Mamdani. Application of fuzzy logic to approximate reasoning using linguistic synthesis. *IEEE T. Computers*, (12):1182–1191, 1977.
- [41] Benoit Mariani, Mayté Castro Jiménez, François JG Vingerhoets, and Kamiar Aminian. On-shoe wearable sensors for gait and turning assessment of patients with parkinson's disease. *IEEE transactions on biomedical engineering*, 60(1):155–158, 2012.

- [42] Connie Marras, Melissa J Armstrong, Christopher A Meaney, Susan Fox, Brandon Rothberg, William Reginold, David F Tang-Wai, David Gill, Paul J Eslinger, Cindy Zadikoff, et al. Measuring mild cognitive impairment in patients with parkinson's disease. *Movement Disorders*, 28(5):626–633, 2013.
- [43] Jerry M Mendel. Uncertain rule-based fuzzy systems. *Introduction and new directions*, page 684, 2017.
- [44] AMS Muniz, H Liu, KE Lyons, R Pahwa, W Liu, FF Nobre, and J Nadal. Comparison among probabilistic neural network, support vector machine and logistic regression for evaluating the effect of subthalamic stimulation in parkinson disease on ground reaction force during gait. *Journal of biomechanics*, 43(4):720–726, 2010.
- [45] Y. Nancy Jane, H. Khanna Nehemiah, and Kannan Arputharaj. A q-backpropagated time delay neural network for diagnosing severity of gait disturbances in parkinson's disease. *Journal of Biomedical Informatics*, 60:169–176, 2016.
- [46] Alice Nieuwboer, René Dom, Willy De Weerdt, Kaat Desloovere, Luc Janssens, and Vangheluwe Stijn. Electromyographic profiles of gait prior to onset of freezing episodes in patients with parkinson's disease. *Brain*, 127(7):1650–1660, 2004.
- [47] Ioannis Pachoulakis and Konstantinos Kourmoulis. Building a gait analysis framework for parkinson's disease patients: Motion capture and skeleton 3d representation. In *2014 International Conference on Telecommunications and Multimedia (TEMU)*, pages 220–225. IEEE, 2014.
- [48] Rajesh Pahwa and Kelly E Lyons. *Handbook of Parkinson's disease*. Crc Press, 2013.
- [49] Song Pan, Serdar Iplikci, Kevin Warwick, and Tipu Z Aziz. Parkinson's disease tremor classification—a comparison between support vector machines and neural networks. *Expert Systems with Applications*, 39(12):10764–10771, 2012.
- [50] Naoshi Saito, Teiji Yamamoto, Yoshihiro Sugiura, Saori Shimizu, and Masaru Shimizu. Lifecorder: a new device for the long-term monitoring of motor activities for parkinson's disease. *Internal Medicine*, 43(8):685–692, 2004.
- [51] Arash Salarian, Heike Russmann, François JG Vingerhoets, Catherine Dehollain, Yves Blanc, Pierre R Burkhard, and Kamiar Aminian. Gait assessment in parkinson's disease: toward an ambulatory system for long-term monitoring. *IEEE transactions on biomedical engineering*, 51(8):1434–1443, 2004.
- [52] Armin Salimi-Badr. It2cfnn: An interval type-2 correlation-aware fuzzy neural network to construct non-separable fuzzy rules with uncertain and adaptive shapes for nonlinear function approximation. *arXiv preprint arXiv:2108.08704*, 2021.
- [53] Armin Salimi-Badr, Mohammad M. Ebadzadeh, and Christian Darlot. Fuzzy neuronal model of motor control inspired by cerebellar pathways to online and gradually learn inverse biomechanical functions in the presence of delay. *Biol. Cybern.*, 111(5-6):421–438, 2017.
- [54] Armin Salimi-Badr and Mohammad Mehdi Ebadzadeh. Backpropagation-free learning method for correlated fuzzy neural networks. *arXiv preprint arXiv:2012.01935*, 2020.
- [55] Armin Salimi-Badr and Mohammad Mehdi Ebadzadeh. A novel self-organizing fuzzy neural network to learn and mimic habitual sequential tasks. *IEEE Transactions on Cybernetics*, pages 1–10, 2020.
- [56] Armin Salimi-Badr, Mohammad Mehdi Ebadzadeh, and Christian Darlot. A possible correlation between the basal ganglia motor function and the inverse kinematics calculation. *Journal of Computational Neuroscience*, 43(3):295–318, 2017.
- [57] Armin Salimi-Badr, Mohammad Mehdi Ebadzadeh, and Christian Darlot. A system-level mathematical model of basal ganglia motor-circuit for kinematic planning of arm movements. *Computers in Biology and Medicine*, 92:78–89, 2018.
- [58] Armin Salimi-Badr and Mohammad Hashemi. A neural-based approach to aid early parkinson's disease diagnosis. In *2020 11th International Conference on Information and Knowledge Technology (IKT)*, pages 23–25, 2020.
- [59] Jooeun Song, Susan Sigward, Beth Fisher, and George J Salem. Altered dynamic postural control during step turning in persons with early-stage parkinson's disease. *Parkinson's Disease*, 2012, 2012.
- [60] BL Su, R Song, LY Guo, and Chen-Wen Yen. Characterizing gait asymmetry via frequency sub-band components of the ground reaction force. *Biomedical Signal Processing and Control*, 18:56–60, 2015.
- [61] Marianne Vaugoyeau, F Viallet, S Mesure, and J Massion. Coordination of axial rotation and step execution: deficits in parkinson's disease. *Gait & posture*, 18(3):150–157, 2003.
- [62] Galit Yoge, Nir Giladi, Chava Peretz, Shmuel Springer, Ely S Simon, and Jeffrey M Hausdorff. Dual tasking, gait rhythmicity, and parkinson's disease: which aspects of gait are attention demanding? *European journal of neuroscience*, 22(5):1248–1256, 2005.

- [63] Galit Yoge, Meir Plotnik, Chava Peretz, Nir Giladi, and Jeffrey M Hausdorff. Gait asymmetry in patients with parkinson's disease and elderly fallers: when does the bilateral coordination of gait require attention? *Experimental brain research*, 177(3):336–346, 2007.
- [64] Wei Zeng, Fenglin Liu, Qinghui Wang, Ying Wang, Limin Ma, and Yu Zhang. Parkinson's disease classification using gait analysis via deterministic learning. *Neuroscience letters*, 633:268–278, 2016.